Frontiers in Nanoscience and Nanotechnology

Research Article ISSN: 2397-6527

Microneedle-assisted delivery of anti-migraine drugs across porcine skin: almotriptan malate and naratriptan hydrochloride

Iqra Ahmad[1], Kevin B Ita[1]*, Matthew J Morra[2] and Inna E Popova[2]

[1]College of Pharmacy, Touro University, Mare Island-Vallejo, California, 94592, USA

[2]Department of Soil and Water Systems, University of Idaho, Moscow, Idaho, 83844-2340, USA

Abstract

Migraine is a common neurological disorder characterized by nausea, vomiting, photophobia, aching, fever, pain and chills. Triptans are selective serotonin agonists which can used to relieve migraine symptoms. Almotriptan malate and naratriptan hydrochloride are currently used for the management of migraine in the form of oral tablets. Oral tablets may be problematic for patients experiencing nausea and vomiting which are often associated with migraine. The microneedle-assisted transdermal drug delivery of these triptans may improve patient compliance. A vertical six-celled, static Franz diffusion cell system was used to conduct in vitro permeation experiments on porcine ear skin to determine the influence of microneedle-assisted transdermal delivery of both almotriptan malate and naratriptan hydrochloride. HPLC-MS analysis was performed using an Agilent 1200 series high performance liquid chromatography system in combination with an Agilent time of flight mass spectrometer (TOF-MS) system model 6230 (Agilent, Santa Clara, CA, USA). A reversed phase liquid chromatography column (Agilent Zorbax Eclipse Plus C18, 100 mm X 2.1 mm, 3.5 µm), was utilized for chromatographic separation. Confocal laser scanning microscopy was used to characterize the depth of the microchannels created after stainless-steel microneedle roller application. Transdermal flux of both triptans was calculated from the linear portion of the cumulative amount of drug permeated versus time curve. The mean passive flux of almotriptan malate was 13.044 ± 0.32 µg.cm^2.h, while the mean flux following microneedle roller application was 11.281 ± 0.22 µg.cm^2.h. The mean flux values for naratriptan hydrochloride for passive and after microneedle roller application was 0.88 ± 0.29 µg.cm^2.h and 4.18 ± 1.39 µg.cm^2.h, respectively. Statistical analysis was performed using the Student's t-test (GradPad Prism 7). A statistically significant difference ($p<0.05$) between microneedle-treated porcine skin samples compared to untreated skin samples was found for the transdermal flux values of naratriptan hydrochloride. Solid stainless-steel microneedle rollers enhanced the transdermal delivery of naratriptan hydrochloride. In contrast, transdermal flux values obtained for almotriptan malate indicate that differences between microneedle-treated and untreated skin samples was not statistically significant ($p>0.05$).

Introduction

Migraine is a common neurological disorder that affects numerous individuals nationwide [1]. Females are three times more likely to suffer from migraine in comparison with males and the disorder is more prevalent in individuals between the ages of 25 and 55 years [2,3]. Symptoms of migraine include: nausea, vomiting, photophobia, aching, fever and chills. Migraines are usually due to cranial vasodilation and/or the release of pro-inflammatory sensory neuropeptides from the trigeminal system [4]. Although not much is known about the etiology of migraine current studies indicate that the pathophysiology of the disorder maybe linked with both neural and vascular mechanisms. Activation of the trigeminovascular system triggers the release of vasodilators which contribute to the headache associated during a migraine [4]. Vasoactive neuropeptides induce vasodilation and are located within the trigeminal neurons. Vasoactive neuropeptides mediating vasodilation include: calcitonin gene-related peptide (CGRP), substance P, and neurokinin A [5]. CGRP is the most critical neuropeptide involved in the generation of migraine [4]. The release of vasoactive neuropeptides from the trigeminal nerve terminals induces inflammatory reactions in the meningeal blood vessels [4]. Further, the association of 5-hydroxytrptamine (5-HT) and migraine pathophysiology is supported by the increasing levels of 5-hydroxyindoleacetic acid, a major metabolite of 5-HT, during a migraine [5].

Increased understanding of the role 5-HT receptors play in regard to migraine has led to the development of new medications such as triptans. Triptans are serotonin 5-HT 1B and 1D receptor agonists and can be used to for the management of migraine [5]. Triptans work by binding to selective serotonin receptors like the 5-HT 1B and 1D receptors [5]. The 5-HT 1B receptors are located in the intracranial blood vessels within smooth muscle cells while the 5-HT 1D receptor is expressed in the trigeminal nerve fibers [4]. The activation of these receptors is believed to produce cranial vasoconstriction and provide pain relief [5]. Triptans have three modes of action which contribute to their anti-migraine effects [6]. These effects include: vasoconstriction of intracranial extracerebral vessels, inhibition of vasoactive neuropeptide release by the trigeminal terminals, and nociceptive neurotransmission inhibition [6].

Triptans are commonly available as tablets for oral administration [7]. However, many migraine patients fail to comply with oral

Correspondence to: Ita KB, College of Pharmacy, Touro University, Mare Island-Vallejo, California, 94592, USA, Tel: +1 [707] 638-5994; Email: kevin.ita@tu.edu

Key words: *migraine, anti-migraine drugs, naratriptan hydrochloride, almotriptan malate*

Received: July 10, 2018; **Accepted:** July 24, 2018; **Published:** July 27, 2018

triptans because oral treatments may be ineffectual for patients who are experiencing nausea, vomiting, and gastric-stasis which are often associated with migraine [6]. This will interfere with the oral drug absorption and even delay the initial use of the oral medication [7]. Due to the limitations of oral triptans transdermal drug delivery will be a more viable option [7]. The long-term goal is to develop a microneedle-assisted transdermal system for the delivery of both triptans: almotriptan malate and naratriptan hydrochloride.

There are several advantages of transdermal drug delivery which include: avoidance of gastrointestinal irritation, prevention of the first-pass effect, and the provision of stable drug plasma concentration over a sustained period of time [5]. In addition, transdermal delivery also provides a pain-free mode of drug administration. However, not all drugs are suitable for transdermal delivery [8]. For a drug to cross the skin barrier and be delivered into the bloodstream, it must have certain physicochemical properties such as low molecular weight, optimal partition and diffusion coefficients, including appropriate temperature and pH [9]. The greatest drawback of transdermal delivery systems is the poor permeability through the stratum corneum [10].

The stratum corneum (SC) is the main penetration barrier in transdermal drug delivery [10]. It is the outermost layer of the epidermis and consists of 15-20 layers of corneocytes which are embedded in a lipid matrix [10,11]. The aqueous pores in the hydrophilic regions of the SC help to facilitate the transcutaneous diffusion of penetrants [12]. There are several ways of overcoming the SC barrier including sonophoresis, iontophoresis, prodrugs, microemulsions and microneedles (MN) [10,13].

MNs are micron-sized needles that can facilitate the skin penetration of medications by creating micropores which increase transdermal diffusion of drugs [14]. The application of MN allows for painless penetration of the SC barrier which is appealing to patients with needle-phobias because MN does not stimulate the nerves associated with pain [11]. A common disadvantage of MN is that only small amount of the drug can be given each time of administration compared to when using hypodermic needles. MN have been fabricated in a range of different sizes, shapes, and materials [8]. There are five different types of MN which include: solid, coated, dissolving, hollow, and hydrogel-forming [10,11,15]. When using solid MN the drug is applied to the skin after creating micro-pores across the skin [11,13]. MN can also be coated with the drug, where the drug is dissolved off and then the MN are removed [11]. MN can be completely dissolving into the skin where the drug is encapsulated within microneedle and released upon insertion into skin [11]. Alternatively, hollow MN can be used to inject liquid drugs into the skin through a needle bore [11,13]. Hydrogel-forming MN facilitate drug delivery by controlled swelling of the MN patch arrays and upon swelling the drug is released [13]. We will be using solid microneedles for the transdermal delivery of almotriptan malate and naratriptan hydrochloride across porcine ear skin. Microneedle-assisted transdermal delivery can potentially enhance the skin permeability for drug compounds and may lead to a statistically significant increase in transdermal flux values for both almotriptan malate and naratriptan hydrochloride.

Almotriptan malate is a sulfonamide triptan which has shown to be effective in treating migraines with or without aura [2]. It is sold under the brand name Axert and has the molecular weight of 333.465 g/mol [16]. Almotriptan malate selectively binds to and activates serotonin 5-HT 1B and 1D receptors, which are localized in the central nervous system [6]. This triggers intracranial blood vessel constriction which relieves the pain associated with a migraine [2]. Similar to other triptans, almotriptan malate induces vasoconstriction by acting on the 5-HT 1B receptors and inhibits nociceptive transmission by activating the 5-HT 1D receptors [3]. Almotriptan malate's effect on nociceptive transmission contributes to the efficacy on pain transmission, but also its effect in improving associated symptoms such as including nausea, vomiting, or photophobia [3]. A transdermal delivery system for almotriptan malate may provide benefits that oral dosage forms do not.

Naratriptan hydrochloride is another triptan drug utilized for the treatment of migraines. The brand name is Amerge and it has the molecular weight of 335.464 g/mol [17]. This triptan acts as a selective agonist for 5-HT 1B and 5-HT 1D receptors involved in mediating vascular constriction which provides pain relief from migraine [2]. Activation of the 5-HT 1B and 5-HT 1D receptors located in the sensory nerves of the trigeminal system results in the inhibition of vasoactive neuropeptide release which helps to relieve migraine symptoms [2]. Naratriptan hydrochloride is well absorbed, with a 74% oral bioavailability and has a long half-life of approximately six hours [7]. This triptan may help improve patient compliance if constructed into a transdermal patch.

Porcine ear skin was used as a substitute for human skin due to similar skin properties. The SC thickness for porcine at 21-25 μm is comparable to the SC thickness for human skin at 10-25 μm [18-20]. Density of hair follicles between porcine skin and human skin was 20/cm^2 and 14-32/cm^2, respectively [19,21]. Porcine skin is inexpensive and has shown prior reliability for in-vitro skin permeation studies [22].

The influence of stainless-steel microneedle rollers on the transdermal delivery of almotriptan malate and naratriptan hydrochloride across pig ear skin in-vitro was studied. It was hypothesized that microneedle-assisted delivery of both triptans will enhance the transdermal flux.

Materials and Methods

Materials

Almotriptan malate, naratriptan hydrochloride, phosphate buffer saline (PBS, pH 7.4) were purchased from Sigma Aldrich Co. (St. Louis, MO, USA). PBS was used as a reconstitution agent for almotriptan malate and naratriptan hydrochloride. The NanoPure Infinity Ultrapure water system (Barnstead, Dubuque, IA, USA) was used to obtain deionized water for all experiments. Stainless-steel microneedle rollers with a density of 192 microneedles and microneedle length of 500 μm were obtained from Pearl Enterprises LLC (Lakewood, NJ USA). Raw porcine ears were purchased from Pel- Freez Arkansas LLC (Rogers, AR, USA) and allowed to thaw at room temperature before experimental use.

Methods

Skin Preparation: The Institutional Animal Care and Use Committee (IACUC) and Institutional Biosafety Committee (IBC) of Touro University, Mare Island-Vallejo, CA, USA approved the experiments. Raw porcine ears were purchased, thawed and carefully shaved using an electric hair clipper. An electric dermatome was utilized (Nouvag®, Goldach, Switzerland) to prepare split-thickness skins and the Digimatic Micrometer (Mitutoyo, Tokyo, Japan) was used to measure the thickness of the porcine samples. The dermatomed skin samples obtained were individually enclosed in aluminum foil and plastic bags and stored at -20 °C until further use.

***In-vitro* Diffusion Studies:** A vertical six-celled Franz diffusion system (PermeGear, Hellertown, PA, USA) was utilized to conduct transdermal permeation studies. The six cells consisted of a top donor compartments and lower receptor compartments. To help maintain uniform drug distribution the receptor cells were magnetically stirred. Each of the six cells also consisted of a sampling port and a circulating water jacket at 37 °C to simulate human body temperature (ThermoFisher Scientific, Waltham, MA, USA). The Franz diffusion cells had a diffusion area of 1.77cm^2 a receptor volume of 12mL filled with PBS.

Microneedle-treated and untreated porcine ear skin samples were used for this experiment. To prepare microneedle-treated samples a stainless-steel microneedle roller was applied to porcine skins to create microchannels. To create microchannels in the skin samples the microneedle roller was applied 15 times to each skin sample in the vertical, diagonal, and horizontal directions. The roller was applied and measured at a force of 20lbs using a weighing scale. Three of six compartments of the Franz diffusion cell system contained microneedle treated skin samples while the remaining three consisted of untreated samples, serving as controls. Porcine ear skins were mounted between the upper donor and lower receptor compartments. Vacuum grease was utilized (Dow Corning, Midland, MA, USA) along with a metal clamp to help hold the porcine samples stay in place and prevent loss of triptan solution. Skin samples were placed with the stratum corneum surface facing towards the donor cell. Diffusion experiments for both triptans were replicated six times each (n=6) and each experiment was conducted out using 1 mL of either almotriptan malate or naratriptan hydrochloride. The triptan was placed on porcine skin samples using 1 mL syringes through the donor compartment. To help reduce evaporation the donor compartments and sampling ports were covered with parafilm and aluminum foil. At intervals of 2 hours for a 12-hour period, 1mL aliquots of the receptor solution were taken using 1 mL syringes. Collected solutions were placed in vials from Agilent Technologies (Agilent, Santa Clara, CA) and stored in 4°C until shipment to the University of Idaho for high performance liquid chromatography-mass spectrometry (HPLC–MS) analysis. After each extraction receptor compartments were refilled with an equal volume of fresh PBS (1mL). Using the collected HPLC-MS data the cumulative amount of drug permeated was plotted as a function of time for both triptans. The slope of the steady state portion of the cumulative amount of drug permeated over time was used to further calculate the transdermal flux values.

HPLC/DAD/TOF-MS Analysis of Pharmaceuticals: Quantitative analysis of the drug concentrations in the samples collected was carried out using HPLC-MS analysis. HPLC-MS analysis was performed using an Agilent 1200 series liquid chromatography system in combination with an Agilent time of flight mass spectrometer (TOF-MS) model 6230 (Agilent, Santa Clara, CA, USA). Chromatographic separation was achieved using a reversed phase liquid chromatography column (Agilent Zorbax Eclipse Plus C18, 100 mm X 2.1 mm, 3.5 µm) with temperatures maintained at 30°C (Agilent, Santa Clara, CA, USA). The mobile phase consisted of 0.1% formic acid in acetonitrile. From 3 to 20% there was a linear gradient in 3 min followed by an increase to 100% in 2 min. Equilibration at 3% was subsequently carried out for 5 min. The mobile phase flow rate was 0.3 mL min^{-1} with an injection volume of 5 µL. The reconstructed ion current mode with a m/z of 336.16 was used to perform quantification of both triptans.

Microchannel Depth Characterization by Confocal Laser Scanning Microscopy (CLSM): CLSM was performed at the Van Winkle Lab housed in the Center for Health and the Environment of the University of California, Davis to characterize the depth of the microchannels created by the stainless-steel microneedle roller. Confocal images were taken of both microneedle-treated and untreated skin samples. After the microneedle roller application, porcine samples were treated with 200 uL of fluorescent dye, Alexaflour 594 (Thermo Fisher Scientific, Waltham, MA, USA). The sample was then blotted with Kimwipes (Kimberly-Clark Professional, Roswell, GA, USA) to remove excess dye. Strips of microneedle-treated porcine skin were cut into sections, embedded with OCT medium (Sakura Finetek Inc., Torrance, CA, USA) and placed onto Tissue-Tek Cryomolds (Sakura Finetek Inc., Torrance, CA, USA). All samples were cryosectioned to 10 µm thick vertical sections using a Leica CM1950 Cryostat (Leica Biosystems, Buffalo Grove, IL, USA) and transferred onto glass slides in preparation for CLSM. Confocal images of microneedle-treated and untreated skin samples taken using a Leica TCS LSI laser scanning confocal microscope. The frame was set at 1024 X 1024 pixels with a magnification of 5X. Excitation was carried out at 590 nm and emission at 617 nm. Untreated porcine samples were also treated with Alexaflour 594, cryosectioned and examined using the Leica TCS LSI confocal laser scanning microscope.

Data Analysis: The transdermal flux of both triptans was determined from the slope of the average cumulative amount versus time curve. For each drug experiments were replicated six times and the dilution of each drug was accounted for by using the Hayton-Chen equation.

$$C_n^1 = C_n\left(\frac{V_T}{V_T - V_S}\right)\left(\frac{C_{n-1}^1}{C_{n-1}}\right)$$

For the Hayton–Chen equation, C_n^1 is the corrected concentration and C_n is the measured concentration in the nth sample. V_T stands for the total volume of the receptor fluid (12 mL) and V_S is the volume of sample withdrawn from the receptor fluid (1 mL). C_{n-1}^1 represents the corrected concentration in (n-1)th sample while C_{n-1} is the measured concentration in (n-1)th sample.

Statistical Analysis: GraphPad Prism 7 (GraphPad Software, Inc., La Jolla, CA, USA) was used to perform statistical analysis. Results with a p-value of less than 0.05 was considered to be statistically significant. To plot the graphs, the average replicates (n=6) with corresponding standard deviation was used for both almotriptan malate and naratriptan hydrochloride (Table 1).

Results

Microchannel Formation

Confocal laser scanning microscopy was used to compare both microneedle-treated and untreated skins. Untreated porcine skin samples were used as controls to compare against microneedle-treated

Table 1. Transdermal flux (µg/cm^2/h ± SD) of naratriptan hydrochloride and almotriptan malate following microneedle roller application. Passive flux values served as controls (n = 6)

Solution Name	Passive (µg/cm^2/h)	Microneedle (µg/cm^2/h)	P- Value
Naratriptan hydrochloride	0.881 ± 0.293	4.187 ± 1.396	0.0054
Almotriptan malate	13.044 ± 0.32	11.281 ± 0.22	0.6053

samples and determine whether microchannels were formed after microneedle roller application. Figure 1A shows the formation of a microchannel after being treated with microneedle rollers. It is visible that the microneedle roller successfully penetrated the stratum corneum to create micropores in the skin which were visible with Alexaflour 594 fluorescent dye. The pore constructed by the microneedle roller is displayed in Figure 1A with a microchannel depth of 215 μm. Unlike Figure 1A, the untreated porcine skin displayed in Figure 1B displays no microchannels.

In-vitro Diffusion Study

Transdermal flux of both naratriptan hydrochloride and almotriptan malate was calculated from the linear portion of the cumulative amount versus time curve. The flux for naratriptan hydrochloride across microneedle-treated pig skin was 4.18 ± 1.39 μg.cm^2.h while the flux for passive diffusion was 0.88 ± 0.29 μg.cm^2.h. There was a statistically significant difference ($p<0.05$) in the transdermal flux values of naratriptan hydrochloride across microneedle-treated porcine samples compared to passive diffusion. Passive penetration rates for naratriptan hydrochloride were low compared to microneedle therefore solid stainless-steel microneedles enhanced the transdermal delivery of this drug. Meanwhile, for the permeation profile of almotriptan malate there was not a statistically significant difference between microneedle-treated and untreated samples. The passive and microneedle-treated flux obtained for almotriptan malate was 13.044 ± 0.32 and 11.281 ± 0.22, respectively (Figure 2).

Discussion

In this paper, the effect of microneedles on the percutaneous transport of almotriptan malate and naratriptan hydrochloride were investigated. Microchannel visualization with confocal microscopy confirmed that the microneedle roller was successfully able to penetrate the skin. Banga, *et al.* reported that the application of a microneedle roller creates microchannels in the skin allowing for enhanced transdermal drug delivery [23]. Methylene blue staining and histological sectioning were used to confirm microchannels while confocal laser scanning microscopy was used to characterize microchannel depth after microneedle roller application [23]. In our project, confocal microscopy images confirmed that the stainless-steel microneedle roller was capable of overcoming the skin barrier to create microchannels across porcine skin [24]. Confocal images comparing microneedle-treated and untreated skin samples indicate that microchannels were created following the application of a microneedle roller (Figure 3). However, despite microchannel formation there was no statistically significant increase in the percutaneous absorption for almotriptan malate. The difference between microneedle-treated and passive flux values of almotriptan malate was not statistically significant ($p<0.05$).

Triptans are commonly taken orally in the form of tablets. Patients with chronic migraine take medications more than once a day [7].

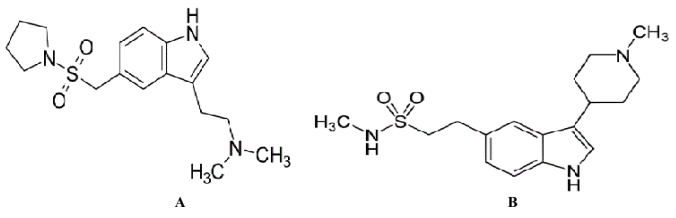

Figure 1. Chemical structures of (A) almotriptan malate and (B) naratriptan hydrochloride

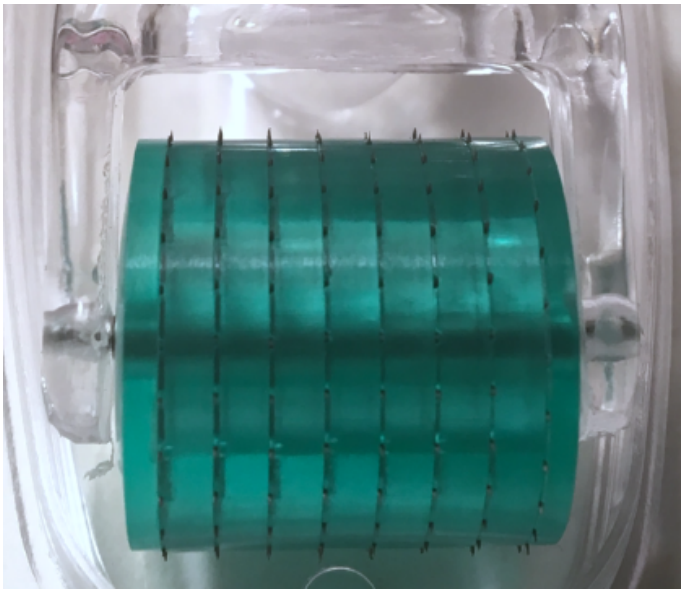

Figure 2. Stainless-steel microneedle roller with microneedles 500 μm in length and density of 192 needles

Almotriptan malate is available in 6.25mg tablets with a maximum daily dosage of 25mg while naratriptan hydrochloride tablets are available in 1mg or 2.5mg tablets with a maximum daily dosage of 5mg [7]. However, due to the symptoms associated with migraine such as pain, vomiting, and nausea many times patients are unable to ingest tablets orally. Other disadvantages include the presystemic metabolism, degradation by enzymes and acid in the stomach, and erratic absorption [8]. Therefore, a microneedle transdermal delivery system would be useful in improving patient compliance. Arya et al. also tested dissolving microneedle patches on human subjects and found that the patches were well tolerated with no pain and swelling, and self-administration rates of microneedle patches were high [25]. A larger phase 1 clinical study conducted on 100 human subjects tested the efficacy of dissolving microneedles to deliver influenza [26]. It was found that the found that vaccine delivery using a microneedle patch was similar to that of when using a hypodermic needle [26]. Needle-phobia is a challenge with many patients and having a microneedle patch would be would be beneficial. Arya et al. also reported that the microneedle patch was preferred by patients over a hypodermic needle [25].

For almotriptan malate, the difference in flux values between microneedle-treated and passive was not statistically significant ($p<0.05$). Several factors may have impacted this occurrence. The effectiveness of a microneedle-assisted transdermal delivery system is dependent on the properties of the skin, the microneedles, and the drug. Since drug entry is imposed by skin permeability the interaction of a specific drug and the skin varies; this is an important factor to be considered. Physiochemical properties of the compound such as molecular weight, drug concentration, pH, melting point, and partition coefficient all influence the rate of transdermal drug delivery. Small molecular weight compounds penetrate at a faster rate that larger ones, therefore having a molecular weight of less than 500 Daltons is typically needed to cross the stratum corneum. The human skin consists of a lipid rich bilayer which makes it necessary for compounds to have both aqueous and lipid solubilities. An ideal transdermal drug delivery candidate would have an aqueous solubility of greater than 1 mg/mL, partition coefficient (log P) between 1-3, point of less than 200 °C [27]. Compounds with log P values below 1 are too hydrophilic to

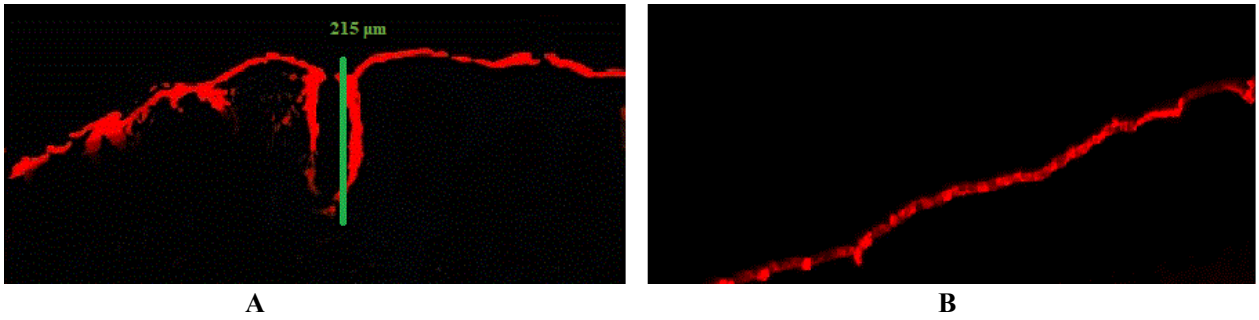

Figure 3. Images of porcine skin samples by confocal laser scanning microscopy (CLSM). (A) Microneedle treated porcine skin showing a single microchannel depth of 215 µm (B) Untreated porcine skin

effectively disrupt the stratum corneum while those greater than 3 are too hydrophobic resulting in low therapeutic plasma concentrations [27]. The melting point of a compound is indirectly proportional to its lipophilicity and solubility in skin lipids [13]. A low melting point will allow for faster penetration and optimal transdermal delivery. Almotriptan malate has a molecular weight of 335.466 Daltons, log P value of 1.6, and a melting point of 170 °C [7]. However, the interactions between the drug, microneedles and the skin are complex. Several investigators have studied the relationship between the physicochemical properties of compounds and skin permeability [28,29]. Only a few variables were studied in the Potts-Guy equation but currently those variables now include properties such as dipole moment and polar surface area [28,29]. Clearly, these are complex interactions worthy of further investigation (Figures 4 and 5)

Microneedle length, density, insertion force and time can all influence the permeation rates of compounds across the skin. A possible explanation of why there was low flux values for microneedle-treated skin samples for almotriptan malate maybe dependent on microneedle length and density. Microneedles that were 500 µm in length were used for this study. Increasing the length may increase the penetration rate of almotriptan malate. In the study by Nalluri, *et al.* 500 µm and 1000 µm microneedles were compared for the in vitro permeation of Levodopa across porcine ear skin [30]. It was found that longer microneedle arrays are able to create pores at a greater [30]. The use of 500 µm microneedle arrays led to a lower permeation rate of levodopa probably due to the inability of the shorter microneedles to create deep enough pores [30]. Another study by Li, *et al.* reported that the microneedle-assisted transdermal delivery effectively increased antibody delivery when microneedle length, microneedle array, and drug concentration were increased [31]. Banga, *et al.* confirmed that an increase in microneedle length from 500 µm to 1100 µm and 1400 µm enhanced microchannel depth [14]. A greater microneedle depth is sometimes associated with increased drug penetration [14]. The results showed that an increase in needle length from 500 µm to 1100 µm and 1400 µm significantly increased microchannel depth in the skin [24]. It is important to consider these factors for future studies as this may assist in enhancing the delivery of almotriptan malate. The study conducted by Calatayud-Pascul, *et al.* confirmed that therapeutic drug levels for almotriptan were obtained using an iontophoresis transdermal delivery system [32]. Iontophoresis uses an electrical current to increase drug penetration through the skin [32]. For iontophoresis, a compound less than 12,000 Daltons can be successfully delivered across the skin whereas for microneedle transdermal drug delivery and ideal candidate must have a much lower molecular weight [13]. Using iontophoresis in combination with microneedles has shown to results in faster drug delivery and permeation rates due to both the micropores creates and

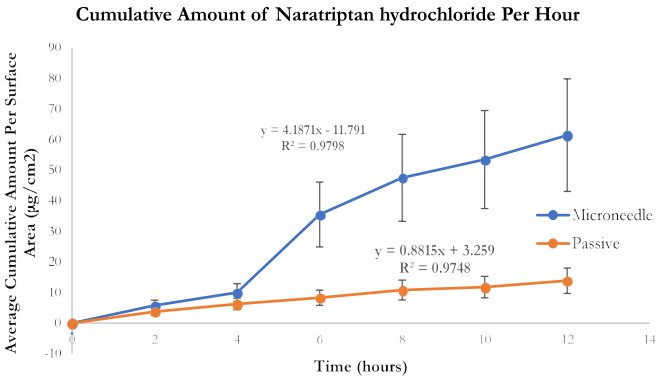

Figure 4. *In-vitro* cumulative amount versus time curve of naratriptan hydrochloride across microneedle-treated and untreated porcine ear skin over 12 hours

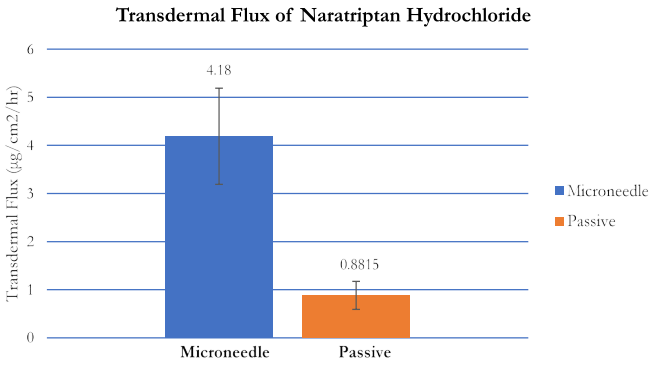

Figure 5. Transdermal flux of naratriptan hydrochloride across microneedle-treated and untreated porcine ear skin over 12 hours

the electrical current pushing the drug into the skin [33]. Possibly increasing the concentration of almotriptan malate can enhance transdermal permeation however that is again limited because of the need for a low molecular weight when using microneedles. Sachdeva et al. found that iontophoresis treatment delivered three times more drug concentration compared to microneedle treatment [33]. The combination of enhancement technologies such as microneedles with iontophoresis may prove to be effective for the transdermal delivery of almotriptan malate.

Furthermore, the low flux levels of almotriptan hydrochloride across microneedle-treated skin samples may have resulted from the "bed of nails" effect. The phenomenon is associated with high microneedle density and close needle-to-needle spacing which reduces the penetration and efficiency of microneedles [34,35]. Yan, *et al.*

studied microneedles densities ranging from 400 to 11,900 needles/cm^2 [36] . Exerting the same force on the microneedle arrays, the study found that arrays with less than 2000 needles/cm^2 increased drug flux greater than higher needle density arrays of 5625 needles/cm^2 [36]. It has been observed that when microneedle density is high the pressure exerted by each microneedle is significantly reduced preventing proper penetration [34]. Applying the same force to a microneedle array of lower density may have allowed for a greater enhancement of drug flux.

Unlike almotriptan malate, skin pretreatment with microneedle rollers helped to enhance transdermal permeation for naratriptan malate. The molecular weight of naratriptan hydrochloride is 371.924 Daltons, it has a log P value is 1.6, and melting point is 246 °C [7]. This indicates that significant amounts of naratriptan hydrochloride can be delivered through the skin barrier with microneedles in comparison to passive permeation. Further in-vitro studies are needed to determine the influence of variables such as drug concentration, microneedle length, density and design, on the transdermal flux of these triptans. Solid stainless-steel microneedle rollers were used for this experiment. Therefore, it would be interesting to compare flux enhancement with different types of microneedles for almotriptan malate transdermal delivery instead of solely using solid microneedle rollers. The combination of microneedles with other techniques such as iontophoresis and sonophoresis may help enhance permeation rates. Future in-vivo studies should be performed to test for the efficiency of a microneedle-assisted transdermal system for both triptans: almotriptan malate and naratriptan hydrochloride (Figures 6 and 7)

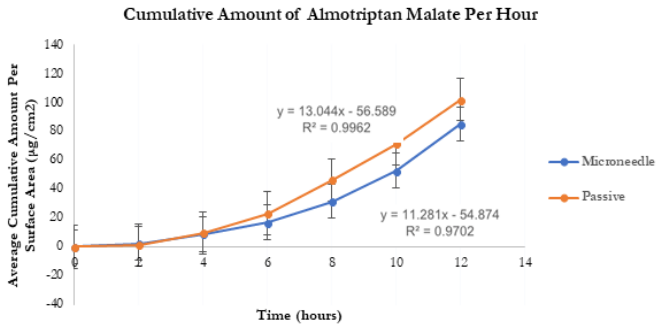

Figure 6. *In-vitro* cumulative amount versus time curve of almotriptan malate across microneedle-treated and untreated porcine ear skin over 12 hours

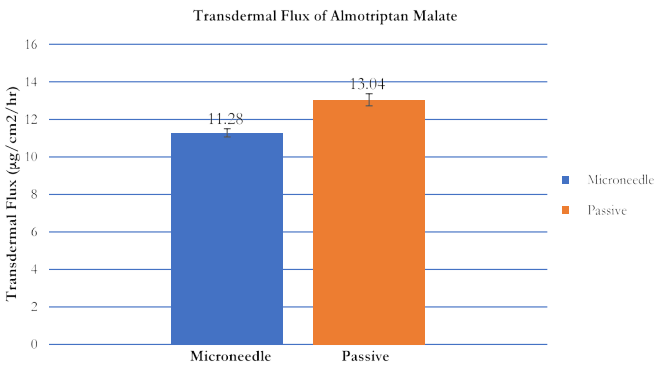

Figure 7. Transdermal flux of almotriptan malate across microneedle-treated and untreated porcine ear skin over 12 hours

Conclusion

This research was carried out to study the influence of microneedles on the transdermal delivery of almotriptan malate and naratriptan hydrochloride. For naratriptan differences in flux values of microneedle-treated and untreated porcine skin samples using solid microneedles were statistically significant ($p<0.05$). Conversely, for almotriptan malate there was not a statistically significant increase in transdermal flux across porcine skin following the application of a microneedle roller ($p>0.05$).

Acknowledgement

We thank Patti Edwards of the Cellular and Molecular Imaging Lab at UC Davis for her assistance with confocal laser scanning microscopy for microchannel visualization images. This work was supported by Touro University California, Vallejo, CA, USA.

Author Contributions

This project was conceptualized by Kevin B. Ita; Diffusion experiments were performed by Iqra Ahmad under the supervision of Kevin B. Ita; LC-MS was conducted by Inna E. Popova; The data was analyzed by Kevin B. Ita and Iqra Ahmad; Matthew J. Morra provided the LC-MS equipment and laboratory; Iqra Ahmad and Kevin B. Ita wrote the paper.

Conflict of Interest

The authors have no conflicts of interest to declare.

References

1. Ingledue VF, Mounsey A (2014) PURLs: treating migraine: the case for aspirin. *J Fam Pract* 63: 94-96. [Crossref]
2. Sandrini G, Perrotta A, Arce Leal NL, Buscone S, Nappi G (2007) Almotriptan in the treatment of migraine. *Neuropsychiatr Dis Treat* 3: 799-809. [Crossref]
3. Wang SJ, Chen PK, Fuh JL (2010) Comorbidities of migraine. *Front Neurol* 1: 16. [Crossref]
4. Aggarwal M, Puri V, Puri S (2012) Serotonin and CGRP in migraine. *Ann Neurosci* 19: 88-94. [Crossref]
5. Pierce MW (2010) Transdermal delivery of sumatriptan for the treatment of acute migraine. *Neurotherapeutics* 7: 159-163. [Crossref]
6. Pini LA, Brovia D (2004) Different characteristics of triptans. *J Headache Pain* 5: 109-111.
7. Adelman JU, Belsey J (2003) Meta-analysis of oral triptan therapy for migraine: number needed to treat and relative cost to achieve relief within 2 hours. *J Manag Care Pharm* 9: 45-52. [Crossref]
8. Ita K (2015) Transdermal Delivery of Drugs with Microneedles-Potential and Challenges. *Pharma* 7: 90-105.
9. Singh I, Morris AP (2011) Performance of transdermal therapeutic systems: Effects of biological factors. *Int J Pharm Investig* 1: 4-9.
10. Prausnitz MR, Langer R (2008) Transdermal drug delivery. *Nat Biotechnol* 26: 1261-1268. [Crossref]
11. Kim YC, Park JH, Prausnitz MR (2012) Microneedles for drug and vaccine delivery. *Adv Drug Deliv Rev* 64: 1547-1568. [Crossref]
12. Larrañeta E, McCrudden MTC, Courtenay AJ, Donnelly RF (2016) Microneedles: A New Frontier in Nanomedicine Delivery. *Pharma Res* 33: 1055-1073.
13. Zaid Alkilani A, McCrudden MTC, Donnelly RF (2015) Transdermal Drug Delivery: Innovative Pharmaceutical Developments Based on Disruption of the Barrier Properties of the stratum corneum. *Pharma* 7: 438-470.
14. Nguyen HX, Banga AK (2015) Enhanced skin delivery of vismodegib by microneedle treatment. *Drug Deliv Transl Res* 5: 407-423. [Crossref]

15. Prausnitz MR (2017) Engineering Microneedle Patches for Vaccination and Drug Delivery to Skin. *Annu Rev Chem Biomol Eng* 8: 177-200.

16. Mathew NT, Finlayson G, Smith TR, Cady RK, Adelman J, et al. (2007) Early Intervention With Almotriptan: Results of the AEGIS Trial (AXERT® Early Migraine Intervention Study). *Headache* 47: 189-198.

17. Maddineni J, Walenga JM, Jeske WP, Hoppensteadt DA, Fareed J, et al. (2006) Product Individuality of Commercially Available Low-Molecular-Weight Heparins and Their Generic Versions: Therapeutic Implications. *Clin Appl Thromb Hemost* 12: 267-276.

18. Abd E, Yousef SA, Pastore MN, Telaprolu K, Mohammed YH, et al. (2016) Skin models for the testing of transdermal drugs. *Clin Pharmacol* 8:163-176.

19. Flaten GE, Palac Z, Engesland A, Filipovic-Grcic J, Vanic Ž, et al. (2015) *In vitro* skin models as a tool in optimization of drug formulation. *Eur J Pharm Sci* 75: 10-24.

20. Lademann J, Richter H, Meinke M, Sterry W, Patzelt A (2010) Which skin model is the most appropriate for the investigation of topically applied substances into the hair follicles? *Skin Pharmacol Physiol* 23: 47-52. [Crossref]

21. Jacobi U, Kaiser M, Toll R, Mangelsdorf S, Audring H, et al. (2017) Porcine ear skin: an in vitro model for human skin. *Skin Res Technol* 13:19-24.

22. Gray GM, Yardley HJ (1975) Lipid compositions of cells isolated from pig, human, and rat epidermis. *J Lipid Res* 16: 434-440. [Crossref]

23. Kalluri H, Kolli CS, Banga AK (2011) Characterization of Microchannels Created by Metal Microneedles: Formation and Closure. *AAPS J* 13: 473-481.

24. Nguyen HX, Banga AK (2015) Enhanced skin delivery of vismodegib by microneedle treatment. *Drug Deliv Transl Res* 5: 407-423. [Crossref]

25. Arya J, Prausnitz MR (2016) Microneedle patches for vaccination in developing countries. *J Control Release* 240: 135-141.

26. Rouphael NG, Paine M, Mosley R, Henry S, McAllister DV, et al. (2017) The safety, immunogenicity, and acceptability of inactivated influenza vaccine delivered by microneedle patch (TIV-MNP 2015): a randomised, partly blinded, placebo-controlled, phase 1 trial. *Lancet* 390: 649-658.

27. Larrañeta E, Lutton REM, Woolfson AD, Donnelly RF (2016) Microneedle arrays as transdermal and intradermal drug delivery systems: Materials science, manufacture and commercial development. *Materials Science and Engineering* 104: 1-32.

28. Moss GP, Gullick DR, Cox PA, Alexander C, Ingram MJ (2006) Design, synthesis and characterization of captopril prodrugs for enhanced percutaneous absorption. *J Pharm Pharmacol* 58: 167-177. [Crossref]

29. Tsakovska I, Pajeva I, Al Sharif M, Alov P, Fioravanzo E (2017) Quantitative structure-skin permeability relationships. *Toxicology* 387: 27-42. [Crossref]

30. Nalluri BNSK, Valluru SSA, Uppuluri CT, Shaik AS (2015) Microneedle Assisted Transdermal Delivery of Levodopa. *Indian Journal of Pharmaceutical Education and Research* 50: 287-294.

31. Li G, Badkar A, Nema S, Kolli CS, Banga AK (2009) *In vitro* transdermal delivery of therapeutic antibodies using maltose microneedles. *Int J Pharma* 368: 109-115.

32. Calatayud-Pascual MA, Balaguer-Fernández C, Serna-Jiménez CE, Del Rio-Sancho S, Femenía-Font A, et al. (2011) Effect of iontophoresis on in vitro transdermal absorption of almotriptan. Int J Pharma 416:189-194.

33. Sachdeva V, Zhou Y, Banga AK (2013) *In vivo* transdermal delivery of leuprolide using microneedles and iontophoresis. *Cur pharma biotech* 14:180-193.

34. Moga KA, Bickford LR, Geil RD, Dunn SS, Pandya AA (2013) Rapidly–Dissolvable Microneedle Patches Via a Highly Scalable and Reproducible Soft Lithography Approach. *Adv Mater* 25: 5060-5066.

35. Gomaa YA, El-Khordagui LK, Garland MJ, Donnelly RF, McInnes F (2012) Effect of microneedle treatment on the skin permeation of a nanoencapsulated dye. *J Pharm Pharmacol* 64: 592-1602. [Crossref]

36. Yan G, Warner KS, Zhang J, Sharma S, Gale BK (2010) Evaluation needle length and density of microneedle arrays in the pretreatment of skin for transdermal drug delivery. *Int J Pharma* 391: 7-12.